COMPACT 8-PORT MIMO ANTENNA FOR C-BAND AND 5G APPLICATIONS

Abstract

In this chapter, a design for 8×8 MIMO antennas with a top edge of 80 mm x 80 mm x 30 mm was proposed. The suggested antenna is 60mm x 60mm x 1.6mm. On a FR4 substrate with a permittivity of 4.4 and a thickness of 0.8 mm, the antenna is printed. The plan was expanded to include 88 MIMO antennas working at WRC 5G. (7.5– 9.5GHz). The operational band of the simulated efficiency is between 47 and 59%. This form factor is ideal for laptop applications due to its good radiation performance and low profile.

Authors

Navneet Singh
Department of Electronics and Communication Engineering
MJP Rohilkhand University
Bareilly, Uttar Pradesh, India
navneetsingh.engg8@gmail.com

Yash Bhardwaj
Department of Electronics and Communication Engineering
MJP Rohilkhand University, Bareilly
Uttar Pradesh, India
yash.bhardwaj.engg@gmail.com

Dr. Hari Kumar Singh
Department of Electronics and Communication Engineering
MJP Rohilkhand University, Bareilly
Uttar Pradesh, India
harsdik@gmail.com

I. INTRODUCTION

This year will see the deployment of fifth generation wireless technology (5G). Presently available 5G mobile phones as well as potential 5G C-band laptops are now available. MIMO technology should be used to increase data transmission speed. Some mobile phone antenna design techniques [1]–[4] have been described for 5G MIMO antenna design, and the majority of them are developed utilising monopoles or slots.

Large bandwidth, large data speeds, and low latency communication are in high demand right now. The standard Long-Term Evolution (LTE) and LTE-advanced (LTE-A) communication systems may not be able to address a number of use cases, Communication systems in the fifth generation (5G) may be able to deliver sufficient bandwidth with low latency. Numerous frequency bands, including the low, mid, and high bands, are being researched for usage in various 5G new radio (NR) use cases. In order to provide a wider coverage than millimetre waves band and a larger bandwidth than the low frequency band to support some 5G use cases, such as mission-critical applications and Enhanced Mobile Broadband, the EU has designated the C-band or mid-frequency band at 3.6GHz (3.4GHz to 3.8GHz) as the primary band for 5G [1]. (eMBB). As a result, a C-band 5G antenna's impedance bandwidth should be approximately 400MHz .

By utilising multiple pathways for data transmission and reception, multiple input multiple output (MIMO) or several antenna deployment technique significantly increases the data throughput, channel capacity, and link reliability in wireless communication systems [2]. For MIMO antennas to provide strong throughput, great spectrum efficiency, and overall superior antenna performance, high isolation is one of the prerequisites (low mutual coupling). Without using additional materials (such decoupling structures) or extending the distance between the antenna elements, antenna designers frequently achieve excellent isolation between the antenna pieces, resulting in a larger antenna and higher production costs.

The suggested antennas must either have a low antenna realised gain (maximum 5dBi) or a constrained bandwidth in order to be suitable for 5G C-band communication systems. Decoupling structures have also been used to lessen the mutual coupling between the antenna parts, increasing the cost of production. A four-element MIMO antenna for sub-6GHz 5G communication systems is described in [3]. To enhance the performance of the antenna, including the mutual coupling between the antenna components, it has been loaded with split-ring resonators (SRRs). It achieves, in turn, a 440MHz bandwidth, 2.98dBi gain, and a -15dB mutual coupling. Although it satisfies the bandwidth requirement, the antenna performance can be enhanced by increasing gain. The utilisation of a four-port MIMO antenna with micro strip feed lines for 5G C-band communication systems is reported in [6]. Gain, 5dBi, -17dB of mutual coupling, and 350MHz are all achieved. Additionally, the bandwidth is 10dB. Although it has a good gain, 400 MHz of bandwidth is needed to cover the 3.4GHz–3.8GHz airwaves set aside for EU nations.

In contrast to previously published research [2–10], the goal of this work is to propose a 5G C-band antenna with a bandwidth of around 400MHz and a greater strength (>5dBi). Additionally, it should increase throughput (-15dB) and mutual coupling (-15dB)

without requiring longer distances between antenna parts or decoupling structures. Therefore, a novel design strategy for an eight-element slotted MIMO antenna with a partial ground plane is suggested. In order to increase bandwidth and satisfy the needs of the 5G C-band communication systems, we applied to properly design and optimise the slots on the patch and ground plane. In addition, it causes the current flow to primarily focus around the feedline, slots, and partial ground plane of the excited antenna element, greatly reducing current flow to other elements and enabling a low mutual coupling to be achieved without the need for a decoupling structure or a longer distance between the antenna elements.

II. ANTENNA DESIGN

Geometry for proposed 8-Port 'MIMO antenna' having two frequency rejection characteristics is shown in Fig.-1.

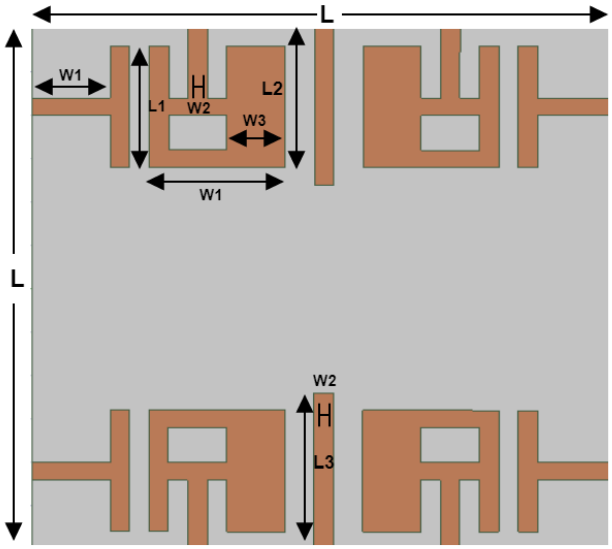

Figure 1: (a): Front of the Antenna

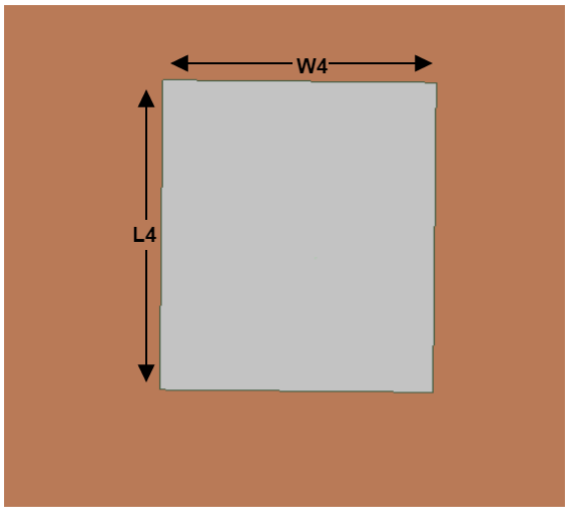

Figure 1: (b): Back of the Antenna

An eight-port "MIMO antenna" with four asymmetric slotted A-shaped patches, four symmetric T-shaped patches, and a modified plane with partial ground is the first step in the design process in order to provide a wide frequency response. For the entire bandwidth, a rectangular sheet with two lines is added to improve impedance matching, isolation, and bandwidth between the two antenna element pairs. The ground plane had SRR placed onto the back of each radiation element, and patch elements had CSRR imprinted on them in order to acquire our results within the frequency range of 7.5 - 9.5GHz.The proposed structure was built on 'FR4-epoxy substrate' having thickness equal to 1.6-mm, with ε_r (dielectric constant) equal to 4.4, tangent loss (δ) equal to 0.0023. The physical dimensions of the proposed '8-Port MIMO antenna', which having small size of 60×60 mm^2, are listed in Table 1.

Table 1: Physical Dimensions of the Antenna

Parameters	h	L	W	L1	W1	L2
Values (mm)	1.6	60.0	60.0	14	6.0	16.0
Parameters	W2	L3	W3	L4	W4	-
Values (mm)	2.0	18	4.0	36.0	28.0	-

III. DISCUSSION AND RESULTS

1. **Scattering parameters for MIMO antenna:** In the following subsection, the Scattering Parameters of the proposed 8-Port 'MIMO antenna' construction includes the terms Reflection Coefficient, Z-Parameters, and Antenna to Antenna Isolation is discussed in depth.

   Reflection coefficient: The modelling and measurement graphs of the reflection coefficient for the proposed MIMO antenna are displayed below. The varied choices for isolation enhancement have resulted in the MIMO antennas having a somewhat different 10 dB bandwidth than the recommended single-element antenna. It is evident that the antenna has excellent impedance matching throughout a wide frequency range between 7.5 and 9.5 GHz, which translates to a fractional bandwidth of 15.9% in relation to the primary operating frequency. Because of the symmetry in the form and placement of each antenna element, each antenna has nearly similar curves for the reflection coefficient. A small difference in the measured reflection coefficients among the antenna elements is due to measurement limitations. The combined result of four ports' reflection coefficient (in dB) is shown in Fig. 2, while the remaining four ports are being isolated.

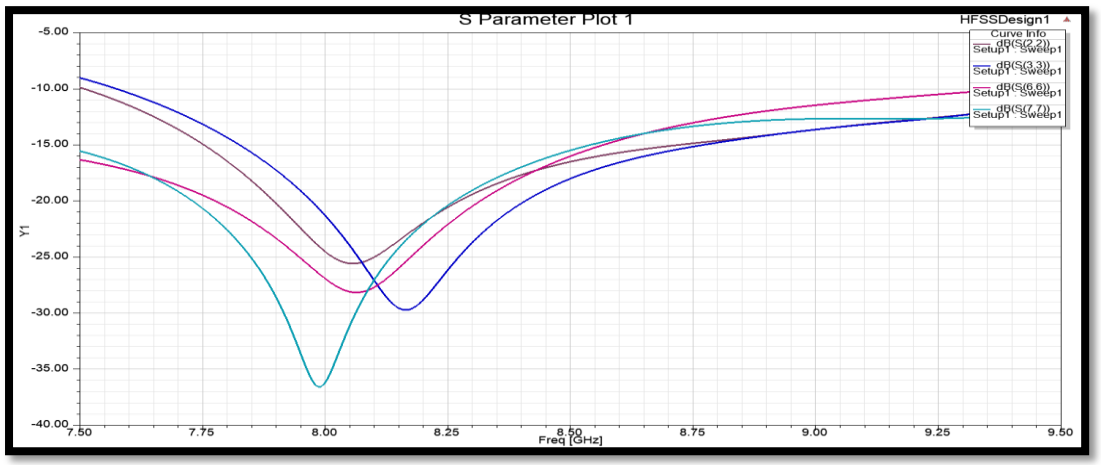

Figure 2: Reflection Coefficient Curve of the Antenna

Z-Parameters: The Z parameter is used to calculate an antenna's quality factor, which can provide information on the achievable bandwidth. Z(ant)=R+jX, where R=R(rad)+R(Loss), allowing you to infer the losses and efficiency in some way. It might be helpful for figuring out an antenna equivalent circuit model. Fig. 3 displays the computed and measured Z-parameter plot of the proposed MIMO antenna.

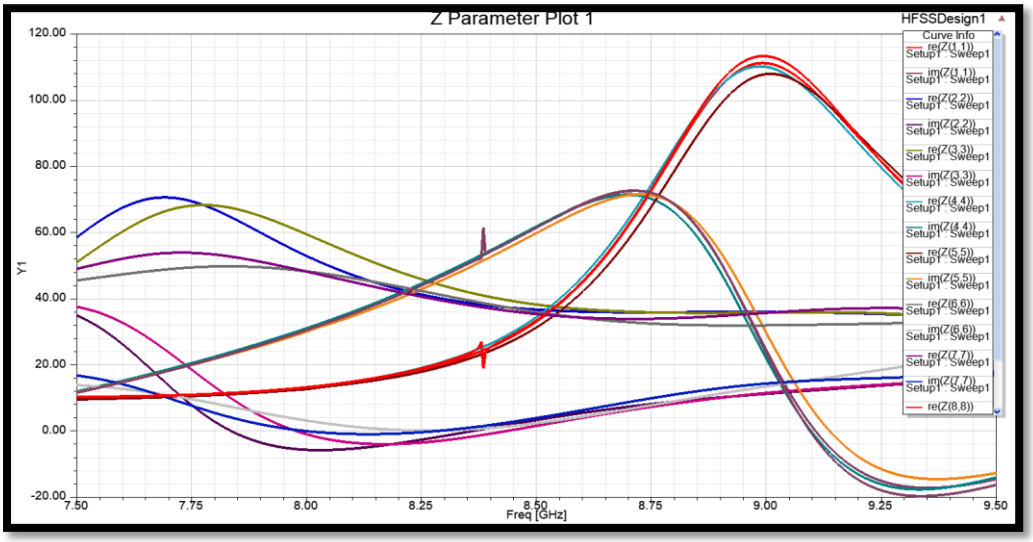

Figure 3: Z-Parameter Curve of the Antenna

Antenna to antenna isolation: The degree to which two antennas are connected is gauged by their isolation from one another. Antenna isolation is often assessed for antennas that are part of the same product, such as the distance between the GPS and WiFi antennas on a smartphone. When offered in this way, the isolation should be as wide as possible.

For antennas that share a common ground plane, such as the diversity and primary cellular antennas on a smartphone, isolation at the lowband can be as low as -10 dB or

less. The isolation will lower the efficiency of both antennas. Figure 4 displays the proposed MIMO antenna's simulated and measured isolation plot.

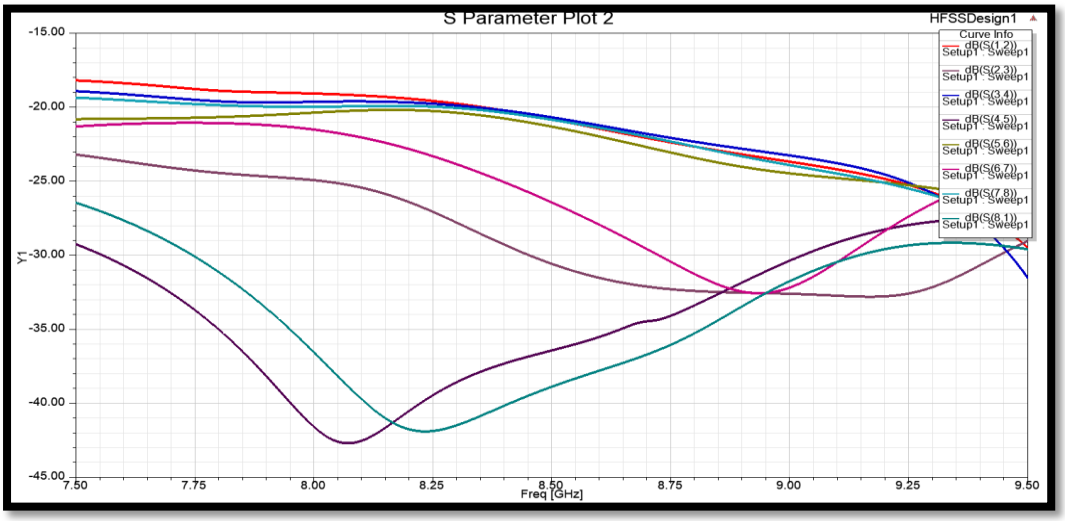

Figure 4: Isolation of the Antenna

2. **Far-Field parameters for MIMO antenna:** In the following subsection, the Far-Field Parameters of the proposed Compact 4-Port 'MIMO antenna' construction include the terms 3-D Polar Plot and gain is discussed in depth.

3-D polar plot: The Polar Plot is a plot that depicts the transfer function of the system G(jω) on a complex plane in polar coordinates. The polar plot representation depicts a plot of magnitude vs. phase angle on polar coordinates with variation in ω from 0 to ∞. The simulated and the measured 3-D Polar plots of the proposed MIMO antenna is shown in Fig.5.

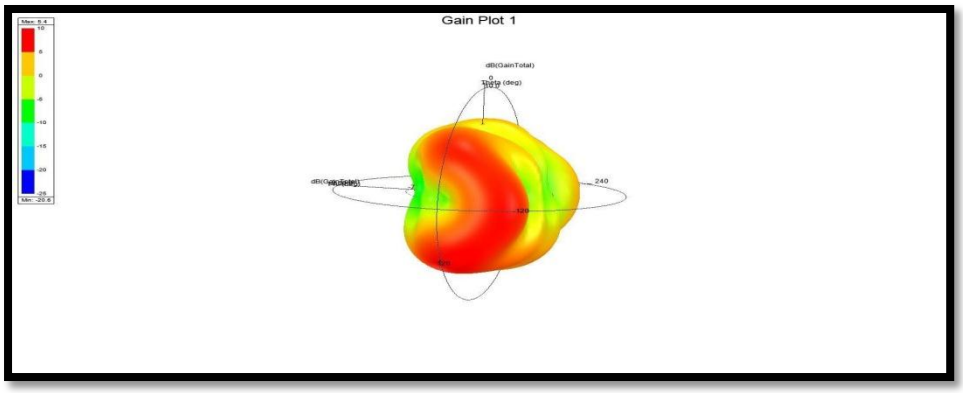

Figure 5: 3-D Polar plot of the Antenna

Gain: That portion of the radiation intensity in a given direction corresponding to a certain polarisation divided by the radiation intensity that would be obtained if the antenna's power was radiated in an isotropic manner. The sum of the partial gains for any

two orthogonal polarizations is the (total) gain of an antenna in a given direction. Losses due to impedance and polarisation mismatches are not included in the gain. If an antenna has no dissipative loss, its gain is equal to its directivity in any given direction. The direction of the highest radiation intensity is assumed if the direction is not provided.

The simulated and the measured gain plot of the proposed MIMO antenna is still working.

3. **Performance parameters of MIMO antenna:** In the following subsection, the performance of the proposed Compact 8-Port 'MIMO antenna' construction includes the terms DG, ECC, TARC, and efficiency is discussed in depth.

Envelope correlation coefficient and diversity gain: 'ECC in-between next to radiation element 1st and 2nd port of N port MIMO antenna system using far-field patterns is given by Equation (1):

$$\mathbf{ECC} = \frac{|\mathbf{S_{11}^{*}S_{12}} + \mathbf{S_{21}^{*}S_{22}}|^{2}}{(\mathbf{1} - |\mathbf{S_{11}}|^{2} - |\mathbf{S_{21}}|^{2})(\mathbf{1} - |\mathbf{S_{22}}|^{2} - |\mathbf{S_{12}}|^{2})}$$

It turns out that the ECC can be completely calculated from the antenna isolation for exceptionally efficient antennas (let's say, >90% or >-1dB). As a result, you can simply measure S_{12} and calculate the ECC without considering the radiation patterns of the antennas. The explanation is that tight coupling will happen if antennas emit the same (or strongly correlated) radiation pattern, without getting into the math (or low isolation). Because antennas are reciprocal, if antenna 1 broadcasts a radiation pattern, antenna 2 will "see" this pattern and receive energy equal to the degree of correlation between the antennas' radiation patterns. Though simple, the reasoning is persuasive.

The following expression specifies the DG of the planned MIMO antenna [19, 20]:

$$DG = 10\sqrt{1 - |\rho|^{2}}$$

where ρ is the coefficient of complex cross-correlation, and $|\rho|$ ≈ECC. Figure 6 and Figure 7 shows the ECC and DG graphs that were simulated and measured. The radiation patterns are used to generate the simulated ECC and DG results, while the S-parameters are used to generate the measured results. As we can understand from Figure 6, the ECC is less than 0.03 for the whole C band, except at the frequency band (7.5 to 9.5 GHz), where the ECC is greater than 1db. As indicated in Figure 7, the DG is larger than 9.95 dB.

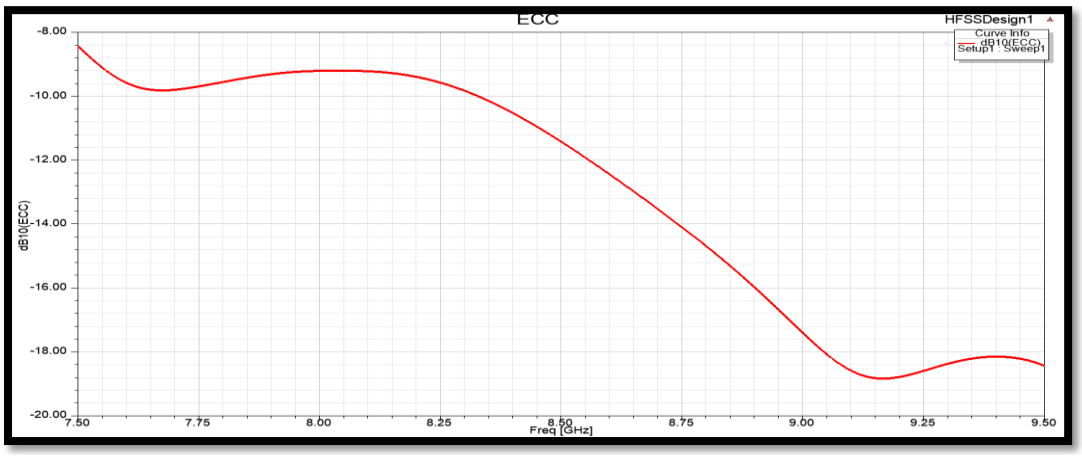

Figure 6: ECC of the Antenna

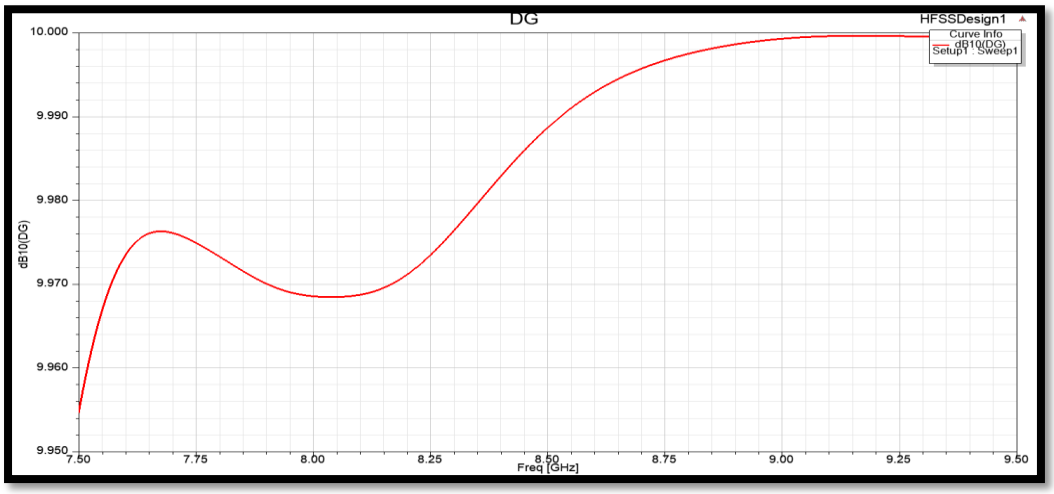

Figure 7: Directive Gain of the Antenna

Efficiency: The high radiation efficiency of over 75 percent backs up the Compact 4-Port MIMO antenna's almost constant performance.

Total active reflection coefficient: 'For a eight-port MIMO system, i = 1,2,3,4,5,6,7,8 j = 2,3,4,5,6,7,8,1 in that order and N = 8, The following equation considers the TARC using the S-parameters [19]:

$$TARC = \sqrt{\frac{|S_{ii} + S_{ij}|^2 + |S_{jj} + S_{ji}|^2}{2}}$$

As seen in Figure 8, this parameter is less than -10 dB over the whole frequency range. The slight disparity between the simulated and observed findings could be related to the effect of soldering the SMA connectors, as well as the tolerance levels for the antenna construction process period.

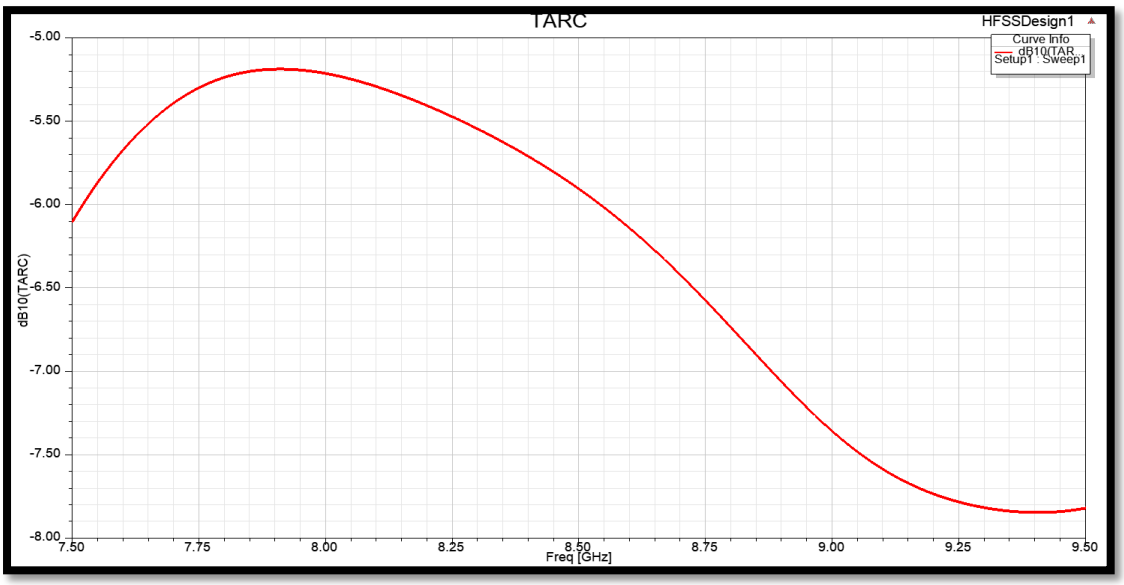

Figure 8: TARC of the Antenna

Voltage Standing Wave Ratio (VSWR): The highest to minimum voltage on a loss-free line is used to establish the voltage standing wave ratio, or VSWR. In reality, every feeder and transmission line experiences a loss. Forward and reverse power are sensed at that system location and translated to a VSWR value in order to measure the VSWR. By doing this, the voltage peaks and minima along the length of the line are not necessary in order to estimate the VSWR at a specific location. All of the antenna's ports' VSWR are displayed in Figure 9 for comparison.

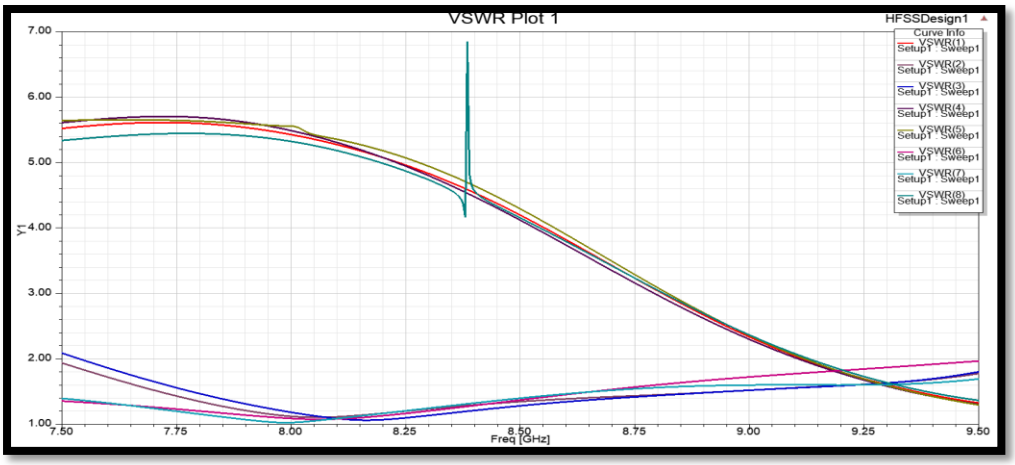

Figure 9: VSWR curve of the Antenna

IV. PERFORMANCE COMPARISON

Table 2 contrasts different existing MIMO systems with the proposed Compact four-port MIMO antenna array in terms of size, isolation between antenna elements, ECC,

operating bands, efficiency, and DG. The proposed 4-port MIMO antenna has excellent ECC and DG values, a short footprint, and a wide impedance bandwidth, as indicated in the table. P.S = proposed structure, DG =Directive Gain, ECC = Envelope correlation coefficient'

Table 2: Performance Comparison of other Antenna with Proposed Antenna

Ref. No.	Year	Number of Ports	Size (mm^3)	Isolation (dB)	ECC	Bandwidth (GHz)	Efficiency (%)	DG (dB)
[21]	2018	2	30×41	< -20	<0.1	2.2 GHz to 5GHz	80	-
[22]	2018	3	58×45	< -15	<0.6	3.1Ghz to 7GHz	80	-
[23]	2021	2	50×50	< -21	<0.04	2.36GHz to 12GHz	-	9.99
[24]	2020	2	32×46	<-20	<0.5	3GHz to 11Ghz	-	-
[25]	2018	1	46×46	<-17	<0.02	-	75	-
[26]	2015	2	40×40	<-15	-	2.3 GHz to 8.8 GHz	-	-
[27]	2015	1	38.5×38.5	<-15	<0.1	2.5 GHz to 12GHz	>75	99
[28]	2014	0	40×40	-	<0.005	2.2 GHz to 13.3GHz	-	8-9.5
[29]	2021	2	48×48	< -18	<0.04	2.5 Hz to 5 GHZ	-	-
[30]	2014	1	50×82	< -15	<0.02	3 GHz to 9GHz	60	-
[31]	2017	1	40×30	< -15	-	2.2GHz to 4.25GHz	58	9.94
P.S	2022	8	60×60	<-10	<0.03	7.5 GHz to 9.5 Ghz	>75	>9.95

V. CONCLUSION

Modern mobile communication systems with great spectrum efficiency rely heavily on multiple input multiple output (MIMO) antennas with pattern diversity. The size of the device, which restricts the number of radiating parts, is a major limiting issue in this technology. This results from maintaining strong isolation between planes. Utilizing this method guarantees the high level of isolation between the ports and can result in directive patterns from each MIMO antenna element. As a result, the final design is appropriate for pattern diversity. The method is used with an IFA antenna, and 6 and 8 element MIMO antennas are simulated and constructed in order to assess the viability of the suggested method. The proposed technique may be validated thanks to the simulation and measurement achieving a good level of agreement. This method may be a strong contender for designing huge MIMO antenna for 5G and C-Band systems. where it is necessary to fit a lot of antennas into a small area.

REFERENCES

[1] J. Y. Deng, J. Yao, D. Q. Sun, and L. X. Guo, "Ten□element MIMO antenna for 5G terminals," Microwave and Optical Technology Letters, vol. 60, Oct. 2018.

[2] H. Zou, Y. Li, C. Y. D. Sim, and G. Yang, "Design of 8 × 8 dual□band MIMO antenna array for 5G smartphone applications," International Journal of RF and Microwave Computer□Aided Engineering, vol. 28, June 2018.

[3] W. Zhang, Z. Weng, and L. Wang, "Design of a dual-band MIMO antenna for 5G smartphone application," 2018 International Workshop on Antenna Technology, pp. 1-3, Mar. 2018.
[4] Z. Qin, W. Geyi, M. Zhang, and J. Wang, "Printed eight-element MIMO system for compact and thin 5G mobile handset", Electronics Letters, Vol. 52, pp. 416-418, Mar. 2016.
[5] W. S. Chen, Y. C. Wu, H. J. Lin, and J. C. Hsu, "Coupled-fed Meandered Loop Antenna for Mobile Phone Applications," 2014 International Symposium on Antennas and Propagation Conference Proceedings, pp. 495-496, Dec. 2014.
[6] W. S. Chen, J. H. You, C. M. Wu, H. T. Chen, and Y. T. Liu, "Coupled-fed meandered loop antenna for USB Dongle Applications," 2014 IEEE International Workshop on Electromagnetics, pp. 82-83, Aug. 2014.
[7] Ramachandran, A., S. Valiyaveettil Pushpakaran, M. Pezholil, and V. Kesavath, "A four-port MIMO antenna using concentric square-ring patches loaded with CSRR for high isolation," IEEE Antennas and Wireless Propagation Letters, Vol. 15, 1196–1199, 2016.
[8] Wang, S. and Z. Du, "Decoupled dual-antenna system using crossed neutralization lines for LTE/WWAN smartphone applications," IEEE Antennas and Wireless Propagation Letters, Vol. 14, 523–526, 2015.
[9] Tiwari, R. N., P. Singh, B. K. Kanaujia, and K. Srivastava, "Neutralization technique based two and four-port high isolation MIMO antennas for UWB communication," AEU-International Journal of Electronics and Communications, Vol. 110, 152828, 2019. [Online]. Available: http://www.sciencedirect.com/science/article/pii/S1434841119311227.
[10] Srivastava, G. and A. Mohan, "Compact MIMO slot antenna for UWB applications," IEEE Antennas and Wireless Propagation Letters, Vol. 15, 1057–1060, 2016.
[11] Lim, J., Z. Jin, C. Song, and T. Yun, "Simultaneous frequency and isolation reconfigurable MIMO PIFA using pin diodes," IEEE Transactions on Antennas and Propagation, Vol. 60, No. 12, 5939– 5946, Dec. 2012.
[12] Lee, J., S. Kim, and J. Jang, "Reduction of mutual coupling in planar multiple antenna by using 1-D EBG and SRR structures," IEEE Transactions on Antennas and Propagation, Vol. 63, No. 9, 4194–4198, Sep. 2015.
[13] Zhai, G., Z. N. Chen, and X. Qing, "Enhanced isolation of a closely spaced four-element MIMO antenna system using metamaterial mushroom," IEEE Transactions on Antennas and Propagation, Vol. 63, No. 8, 3362–3370, Aug. 2015.
[14] Zhao, L. and K. Wu, "A dual-band coupled-resonator decoupling network for two coupled antennas," IEEE Transactions on Antennas and Propagation, Vol. 63, No. 7, 2843–2850, Jul. 2015.
[15] Yuan, Y., K. Zhang, X. Ding, B. Ratni, S. N. Buroker, and Q. Wu, "Complementary transmissive ultra-thin meta-deflectors for broadband polarization-independent refractions in the microwave region," Photon. Res., Vol. 7, No. 1, 80–88, Jan. 2019.
[16] Zhang, K., Y. Yuan, X. Ding, B. Ratni, S. N. Buroker, and Q. Wu, "High-efficiency metalenses with switchable functionalities in the microwave region," ACS Applied Materials & Interfaces, Vol. 11, No. 31, 28423–28430, 2019.
[17] Kim, K. H. and J. E. Schutt-Aine, "Analysis and modeling of hybrid planar-type electromagnetic bandgap structures and feasibility study on power distribution network applications," IEEE Transactions on Microwave Theory and Techniques, Vol. 56, No. 1, 178–186, Jan. 2008.
[18] Ryu, J. and H. Kim, "Compact MIMO antenna for application to smart glasses using T-shaped ground plane," Microwave and Optical Technology Letters, Vol. 60, No. 8, 2010–2013, 2018.
[19] Lin, K., C. Wu, C. Lai, and T. Ma, "Novel dual-band decoupling network for two-element closely spaced array using synthesized microstrip lines," IEEE Transactions on Antennas and Propagation, Vol. 60, No. 11, 5118–5128, Nov. 2012.
[20] Su, S., C. Lee, and F. Chang, "Printed MIMO-antenna system using the neutralization-line technique for wireless USB-dongle applications," IEEE Transactions on Antennas and Propagation, Vol. 60, No. 2, 456–463, Feb. 2012.

[21] Gorai, A., A. Dasgupta, and R. Ghatak, "A compact quasi-self-complementary dual band-notched UWB MIMO antenna with enhanced isolation using Hilbert fractal slot," AEU — Int. J. Electron. Commun., Vol. 94, No. June, 36–41, 2018.

[22] Jaglan, N., S. D. Gupta, B. K. Kanaujia, S. Srivastava, and E. Thakur, "Triple band-notched DG CEBG structure-based UWB MIMO/diversity antenna," Progress In Electromagnetics Research C, Vol. 80, 21–37, 2018.

[23] Zhou, J. Y., Y. F. Wang, J. M. Xu, and C. Z. Du, "A CPW-fed UWB-MIMO antenna with high isolation and dual band-notched characteristic," Progress In Electromagnetics Research M, Vol. 102, No. January, 27–37, 2021.

[24] Zhang, J., L. Wang, and W. Zhang, "A novel dual band-notched CPW-fed UWB MIMO antenna with mutual coupling reduction characteristics," Progress In Electromagnetics Research Letters, Vol. 90, No. December, 21–28, 2020.

[25] Debnath, P., A. Karmakar, A. Saha, and S. Huda, "UMB MIMO Slot antenna with Minkowski fractal shaped isolators for isolation enhancement," progress In Electromagnetics Research M, Vol. 75, No. September, 69–78, 2018.

[26] Zhu, J., B. Feng, B. Peng, S. Li, and L. Deng, "Compact CPW UWB diversity slot antenna with dual band-notched characteristics," Microw. Opt. Technol. Lett., Vol. 55, No. 11, 2562–2568, 2015.

[27] Kang, L., H. Li, X. Wang, and X. Shi, "Compact offset microstrip-fed MIMO antenna for band-notched UWB applications," IEEE Antennas Wirel. Propag. Lett., Vol. 14, 1754–1757, 2015, DOI: 10.1109/LAWP.2015.2422571.

[28] Mao, C. X., and Q. X. Chu, "Compact radiator UWB-MIMO antenna with dual polarization," IEEE Trans. Antennas Propag., Vol. 62, No. 9, 4474–4480, 2014, DOI: 10.1109/TAP.2014.2333066.

[29] Mohan Reddy, S. S., B. Sanjay, K. Aruna Kumari, B. T. P. Madhav, and B. Prudhvi Nadh, "MIMO dual-sensing antenna with notch characteristics," J. Phys. Conf. Ser., Vol. 1804, No. 1, 012194, 2021, DOI: 10.1088/1742-6596/1804/1/012194.

[30] Gao, P., S. He, X. Wei, Z. Xu, N. Wang, and Y. Zheng, "Compact printed uwb diversity slot antenna with 5.5-GHz band-notched characteristics," IEEE Antennas Wirel. Propag. Lett., Vol. 13, 376–379, 2014.

[31] Toktas, A., "G-shaped band-notched ultra-wideband MIMO antenna system for mobile terminals," IET Microwaves, Antennas Propag., Vol. 11, No. 5, 718–725, 2017, DOI: 10.1049/iet-map.2016.0820.

